Supplementary Information for

Harnessing tipping points in complex ecological networks

Junjie Jiang, Alan Hastings, and Ying-Cheng Lai

Corresponding author: Y.-C. Lai (Ying-Cheng.Lai@asu.edu)

Journal of the Royal Society Interface

CONTENTS

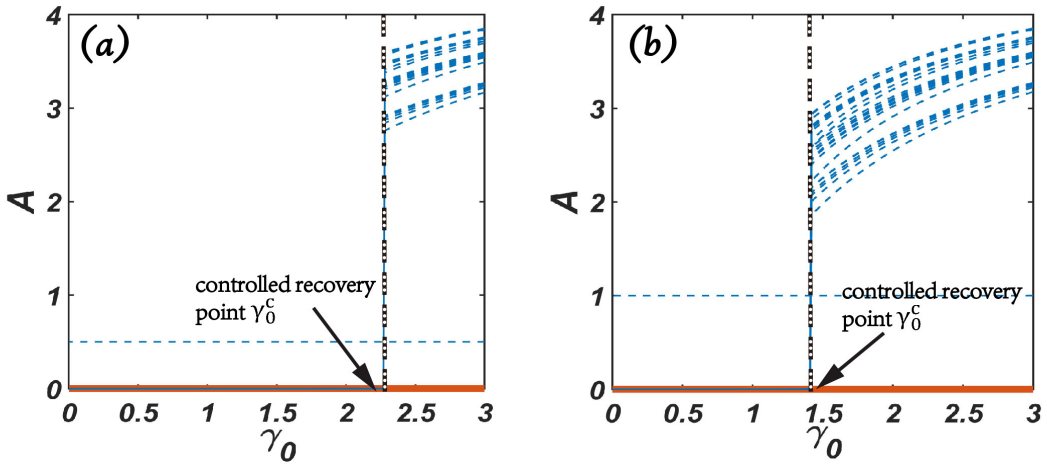

FIG. S1. **Effect of maintained abundance level of the target species on species recovery for a mutualistic network**. For network *B* described in the main text, for two different and relatively low values of the managed abundance of the target species (horizontal dashed line - these values should be compared with the corresponding value of about 4.0 in Fig. 1 in the main text): 0.5 for (a) and 1.0 for (b), successful recovery of all species as the average mutualistic interaction strength γ_0 is increased. Initially, the whole system is in an extinction state with near zero abundances. The data points plotted are the steady state abundance values of all the pollinator species. As predicted by the mathematical analysis in the main text, the level of maintained abundance does have an effect on the recovery point γ_0^c: a smaller value of the level leads to a larger value of γ_0^c. Without abundance management, species recovery is ruled out, as indicated by the thick blue lines at $A = 0$ for both panels. All other parameters have the same values as those in Fig. 1 in the main text.

I. EFFECT OF MAINTAINED ABUNDANCE LEVEL OF THE TARGET SPECIES ON RECOVERY

In Fig. 1 in the main text, the maintained abundance level of the target species for each pollinator-plant mutualistic network is set to a relatively high value. Figure S1 shows, for one of the networks, that a reduction in the level does not impede species recovery.

II. CONTINUOUS EXTINCTION AND RECOVERY PROCESSES IN THE REGIME OF WEAK INTRINSIC GROWTH

In Figs. 4(e-g) in the main text, the gradual extinction of species occurs in the regime when the intrinsic growth rate α of the pollinator species is positive and near zero. The dynamical analysis of the reduced model in the main text indicates that, when the value of α is decreased from a small positive to a negative value, the value of the HSSS moves continuously from the positive to the negative side. Thus, when the value of α is slightly positive, the species abundances gradually decrease to zero as the mutualistic interaction parameter γ_0 decreases to zero. Simulations of empirical networks reveal essentially the same behaviors, as illustrated in Fig. S2 for networks *A* and *B*, providing further support for the ability of the reduced model to capture the essential dynamical features of the high-dimensional mutualistic networks in the real world.

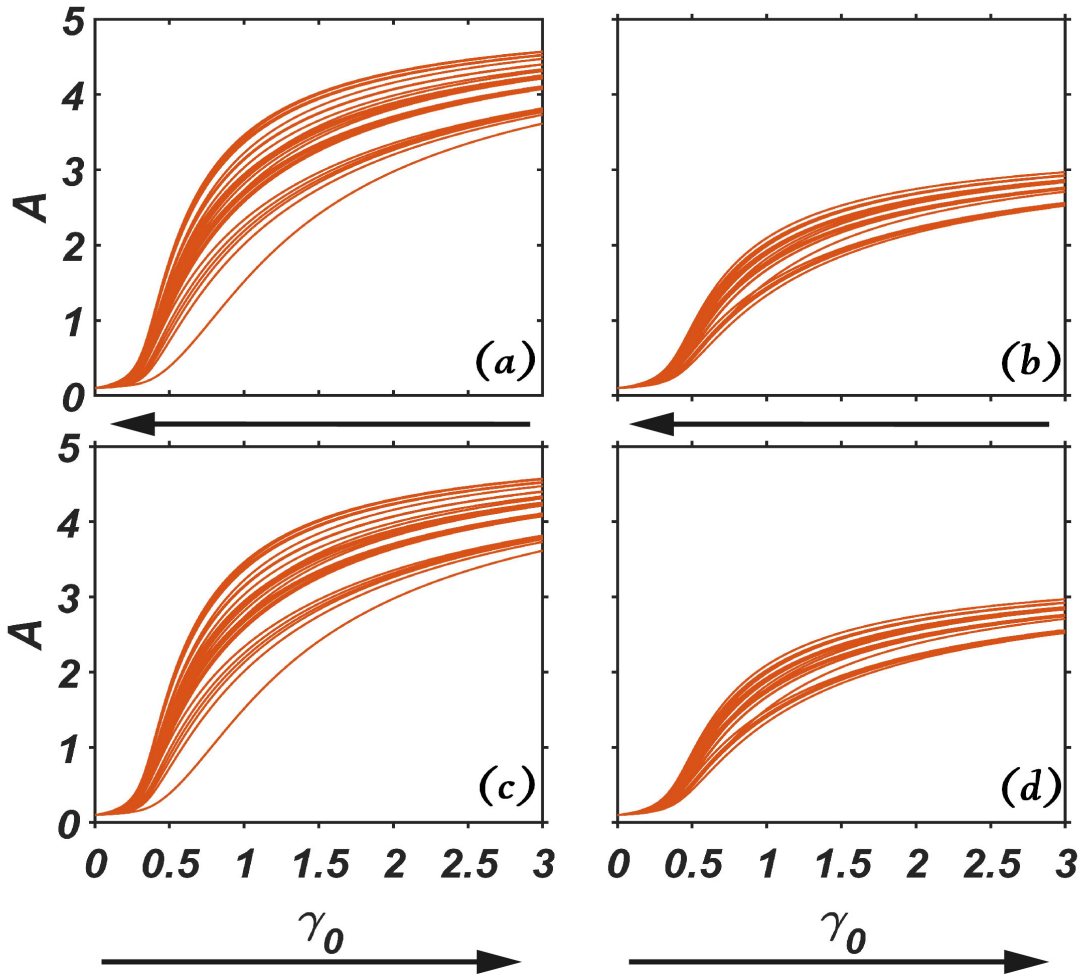

FIG. S2. *Species extinction and recovery as continuous processes in pollinator-plant mutualistic networks*. The systems illustrated are empirical networks A and B as described in the main text, and the continuous extinction and recovery processes occur in the regime of small and positive values of the intrinsic growth rate of the pollinator species. (a,b) In the absence of abundance management (brown curves), extinction of species occurs one after another in a "continuous" fashion for networks A and B, respectively, as the bifurcation parameter γ_0 is decreased from a relatively large value to zero. (c,d) When the value of γ_0 is increased from zero, each species recovers exactly at its point of extinction. The parameter values are $h = 0.2$, $t = 0.5$, $\beta_{ii}^{(A)} = \beta_{ii}^{(P)} = 1$, $\beta_{ij}^{(A)} = \beta_{ij}^{(P)} = 0$, $\alpha_i^{(A)} = \alpha_i^{(P)} = 0.1$, and $\mu_A = \mu_P = 0.0001$. The recovery dynamics can be predicted by the reduced model, as shown in Fig. 4(g) in the main text.

III. STABLE, UNSTABLE STEADY STATES AND THEIR STABILITY OF THE REDUCED MODEL WITH PARAMETER VARIATIONS

Figure S3 provides the results from a detailed stability analysis of the HSSS and USS of the reduced model constructed based on the parameters of the empirical network B in the main text. The eigenvalues of the HSSS are all negative, but the two eigenvalues of the USS have opposite signs, indicating that it is a saddle fixed point in the reduced two-dimensional system.

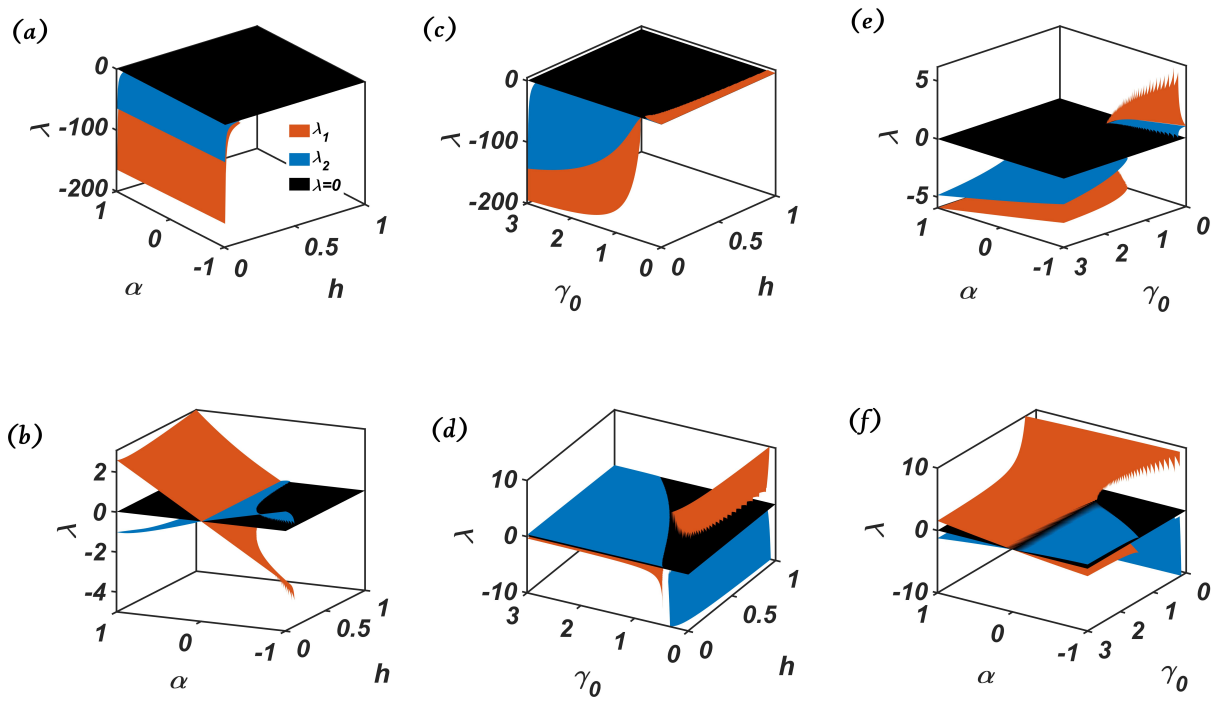

FIG. S3. *Stability of the steady states of the reduced model with parameter* γ_0 *and other parameters variation.* (a-f) The brown and light blue surfaces correspond to, respectively, the two eigenvalues of the Jacobian matrix evaluated at the steady states of the reduced model derived from network B based on Eq. (S5.12), where the black plane provides the zero value reference. Shown in different panels are the eigenvalues of HSSS and USS of the reduced model versus, respectively, (a,b) α and h for $\gamma_0 = 1$, (c,d) γ_0 and h for $\alpha = -0.3$, and (e,f) γ_0 and α for $h = 0.2$. Other parameter values are $t = 0.5$, $\mu = 0.0001$, and $\beta = 1$.

Because of the interspecific competitions in the empirical networks, it is necessary to use Eq. (S4.6) to calculate the effective intraspecific and interspecific competition rates. The steady state solutions of Eq. (S5.19) are given by

$$P' = \left[\alpha + \frac{\langle\gamma_P\rangle A'}{1 + h\langle\gamma_P\rangle A'}\right]\beta_P^{-1}, \tag{S3.1}$$
$$A' = \left[\alpha - \kappa + \frac{\langle\gamma_A\rangle P'}{1 + h\langle\gamma_A\rangle P'}\right]\beta_A^{-1},$$

and the algebraic equation of A' becomes

$$q_1 A'^2 + q_2 A' + q_3 = 0, \tag{S3.2}$$

where

$$\begin{aligned}
q_1 &= -(\beta_A\beta_P h\langle\gamma_P\rangle + \beta_A h\langle\gamma_A\rangle\langle\gamma_P\rangle + \beta_A h^2\alpha\langle\gamma_A\rangle\langle\gamma_P\rangle),\\
q_2 &= -\beta_A\beta_P - h\alpha\beta_A\langle\gamma_A\rangle + h\alpha\beta_P\langle\gamma_P\rangle + \langle\gamma_A\rangle\langle\gamma_P\rangle\\
&\quad + 2h\alpha\langle\gamma_A\rangle\langle\gamma_P\rangle + h^2\alpha^2\langle\gamma_A\rangle\langle\gamma_p\rangle\\
&\quad - \kappa(h\beta_P\langle\gamma_P\rangle + h\langle\gamma_A\rangle\langle\gamma_P\rangle + h^2\alpha\langle\gamma_A\rangle\langle\gamma_P\rangle),\\
q_3 &= \alpha\beta_P + \alpha\langle\gamma_A\rangle + h\alpha^2\langle\gamma_A\rangle - \kappa(\beta_P + h\alpha\langle\gamma_A\rangle),
\end{aligned}$$

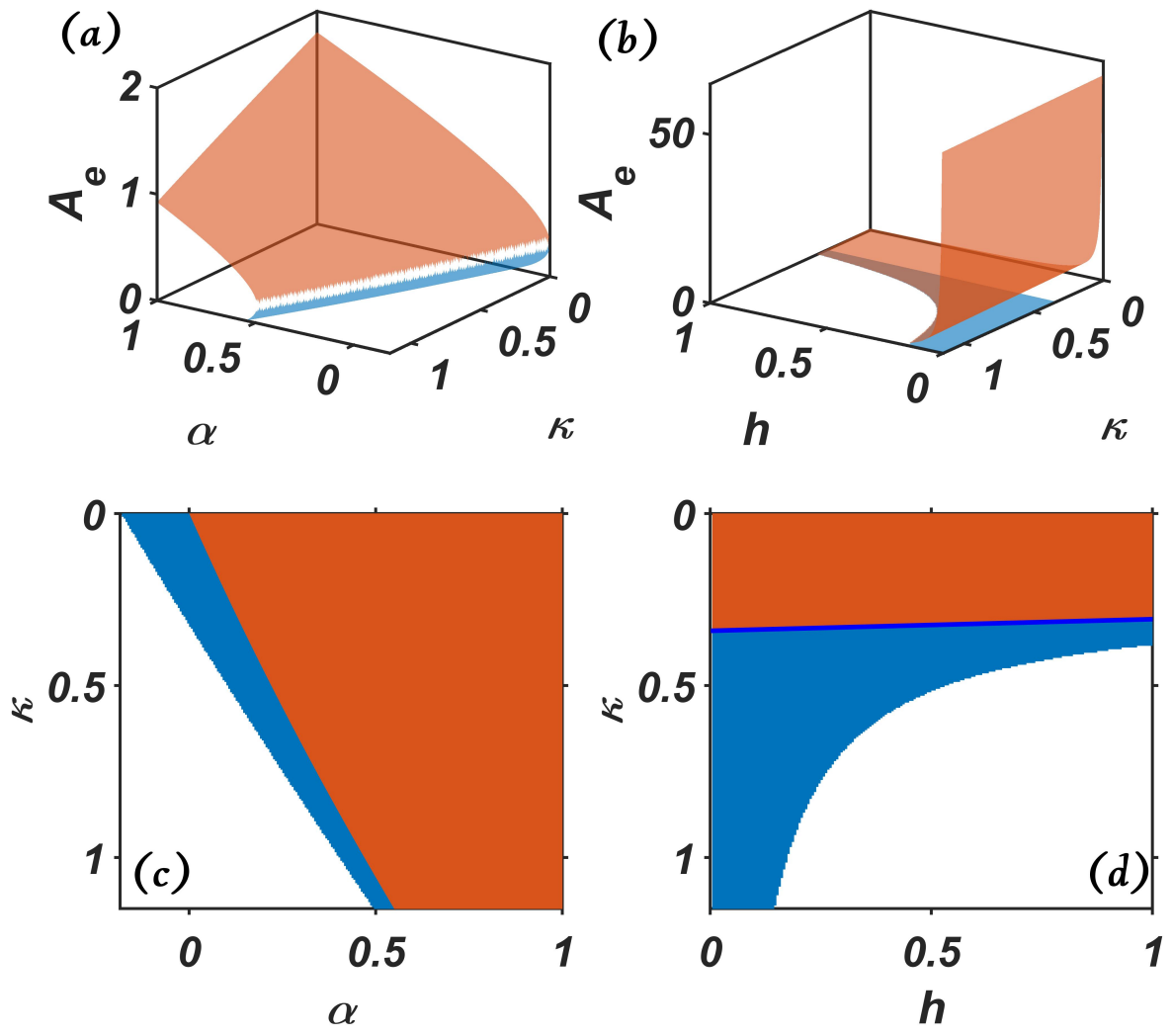

FIG. S4. *Stable and unstable steady states of the reduced model.* The reduced model is constructed based on the parameters of the empirical network B described in the main text, where the brown and light blue surfaces correspond to the HSSS and USS, respectively. Shown is the pollinator species abundance of the reduced model versus (a,c) α and κ for $h = 0.4$, and (b,d) h and κ for $\alpha = 0.15$. Other parameters are $t = 0.5$, $\mu = 0.0001$, and $\gamma 0 = 1$. Panels (c,d) are the bottom views of panels (a,b), respectively. The plant abundance can be obtained from the pollinator abundance according to the relation $P_e = \alpha + (\langle\gamma_P\rangle A_e)/(1 + h\langle\gamma_P\rangle A_e)$. In (d), the blue line indicates the movement of the USS from the positive to the negative side as the value of κ is decreased from one to zero.

Using the equation S3.2, we can calculate the HSSS and USS as shown in Fig. S4. The effective pollinator abundance A_e of the reduced model can explain why management can recover the mutualistic system and remove the hysteresis phenomenon. Figures S4(a-d) show that the HSSS and USS have positive values. In Fig. S4(b), The light blue region has positive HSSS and USS values, while in the brown region, HSSS is positive and USS is negative. In the white region, the HSSS and USS solutions are complex, which are ecologically not realistic. As shown in Fig. S4,the parameter region of α and κ with positive USS values is much smaller than that with positive HSSS

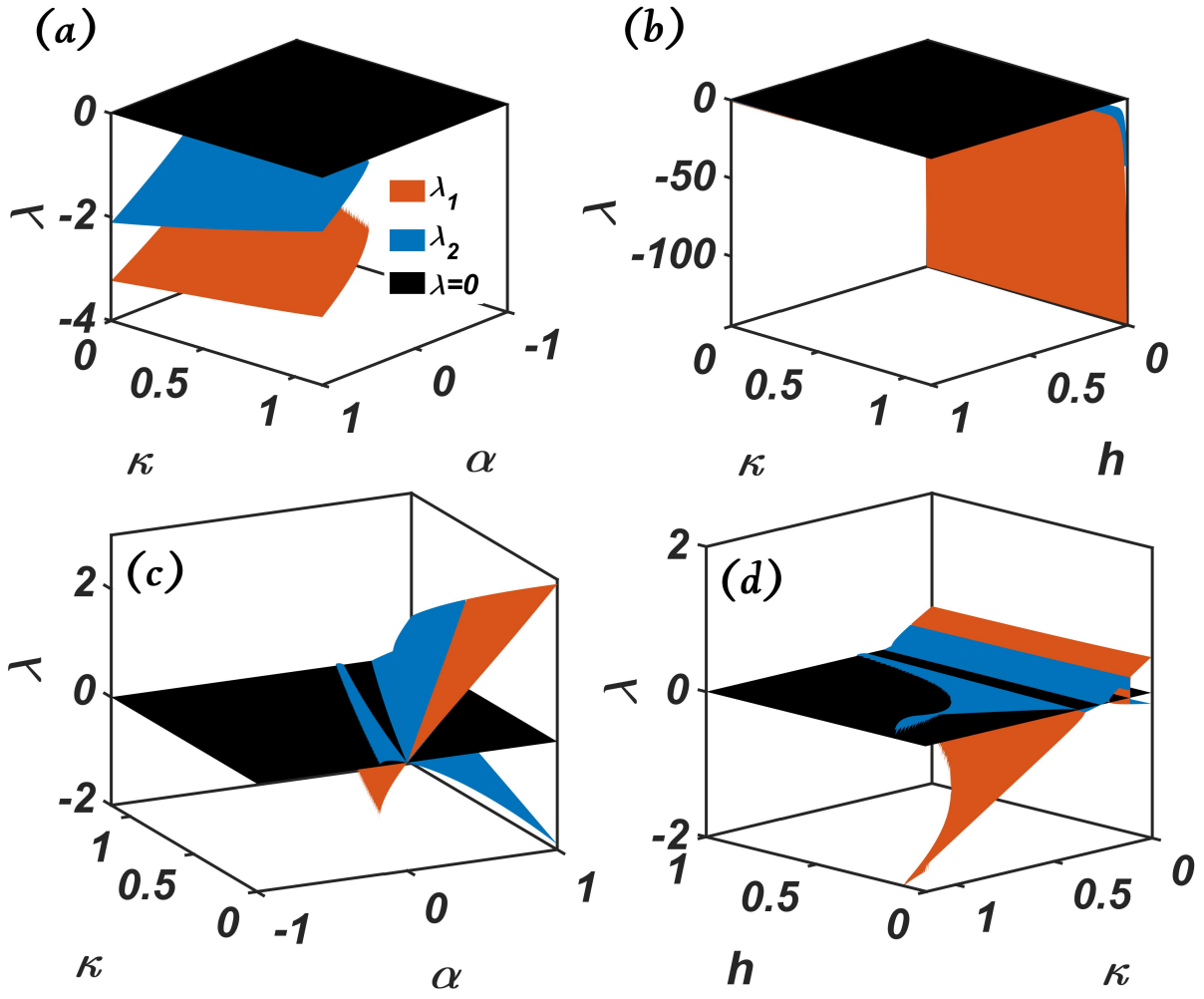

FIG. S5. *Stability of the steady states of the reduced model versus the pollinator decay rate* κ *and other parameters*. Shown are the two eigenvalues (brown and light blue surfaces) of the Jacobian matrix evaluated at the steady state of the reduced model constructed from the empirical network B. The eigenvalues of the HSSS and USS versus, respectively, (a,c) α and κ for $h = 0.4$, and (b,d) h and κfor $\alpha = 0.15$. Other parameters are $t = 0.5$, $\mu = 0.0001$, and $\gamma 0 = 1$.

values. As a result, when the value of κ is increased from zero to 1.15 for $\alpha \in [-0.185, 0.545]$, there exists a region with positive HSSS and USS values, and two transitions in κ: one separating the real from the complex USS solutions, and another separating the positive from the negative USS values. In Fig. S4(d), there are also three regions defined by two transitions. In all cases, a positively valued USS exists, indicating that controlled maintenance of a single, relatively large abundance pollinator species can recover the mutualistic system and remove the hysteresis in Fig.3 in main text.

The results of a stability analysis of the HSSS and USS solutions through the eigenvalues of the Jacobian matrix are presented in Fig. S5.

IV. DIMENSION REDUCTION FOR COMPLEX MUTUALISTIC NETWORKS SUBJECT TO CONTROL

In Ref. [1], an effective 2D model for arbitrary mutualistic networks in the absence of management was derived. Here we extend the dimension reduction approach to networks subject to abundance management. Some general considerations are the following. We assume there is a qualitative correspondence between the mutualistic interaction parameter γ_0 and the state of the environment in that a deteriorating environment for species leads to a decreased value of γ_0. As described in the main text, as γ_0 is decreased from a value at which the species abundances are stable and "healthy," a tipping point can occur at which the populations of all species collapse to near zero values, driving the system into extinction. As γ_0 is increased from a value associated with extinction, when abundance management is present, the system is able to recover. The recovery point is the critical value of γ_0 above which all species abundances have non-zero values. For simplicity, we also assume that the decay parameters for all the pollinators have an identical value: $\kappa_i \equiv \kappa$. There is a qualitative correspondence between κ and the state of the environment in that a deteriorating environment for species implies an increased value of κ. Increasing the value of κ can also lead to a tipping point.

Given a high-dimensional mutualistic network, the reduced dynamical system contains two coupled ODEs: one for all pollinator species except the one under management and another for the plant species. The basic idea of dimension reduction is to quantify the network structure by an effective parameter. The process consists of the following three steps.

We first obtain the effective (average) abundances of the plant and pollinator species. From Eq. (1) in the main text, we have

$$\alpha_i^{(P)} P_i \cong \alpha P_e \ \text{ and } \ \alpha_i^{(A)} A_i \cong \alpha A_e, \tag{S4.3}$$

where P_e and A_e are the effective abundances of the plant and the pollinator species, respectively. Secondly, since species do not out-compete each other when mutualistic partners are absent [2], intraspecific competitions are usually stronger than the interspecific competitions, leading to

$$\beta_{ii}^{(P)} \gg \beta_{ij}^{(P)} \ \text{ and } \ \beta_{ii}^{(A)} \gg \beta_{ij}^{(A)}. \tag{S4.4}$$

For simplicity, we neglect interspecific competitions. The terms describing species competitions in Eq. (1) in the main text can then be written as

$$\sum_{j=1}^{S_P} \beta_{ij}^{(P)} P_i P_j \approx \beta_{ii}^{(P)} P_i^2 \cong \beta P_e^2 \ \text{ and } \ \sum_{j=1}^{S_A} \beta_{ij}^{(A)} A_i A_j \approx \beta_{ii}^{(A)} A_i^2 \cong \beta A_e^2. \tag{S4.5}$$

However, the weak interspecific competitions can be taken into account by writing the species competition terms in Eq. (1) in the main text as

$$\sum_{j=1}^{S_P} \beta_{ij}^{(P)} P_i P_j \cong \frac{\sum_{i=1}^{S_P}\sum_{j=1}^{S_P} \beta_{ij}^{(P)}}{\sum_{i=1}^{S_P} 1} P_e^2 = \beta_P P_e^2 \ \text{ and } \ \sum_{j=1}^{S_A} \beta_{ij}^{(A)} A_i A_j \cong \frac{\sum_{i=1}^{S_A}\sum_{j=1}^{S_A} \beta_{ij}^{(A)}}{\sum_{i=1}^{S_A} 1} A_e^2 = \beta_A A_e^2. \tag{S4.6}$$

We treat the mutualistic strength for every single species:

$$\sum_{j=1}^{S_P} \gamma_{ij}^{(A)} P_j = \sum_{j=1}^{S_P} \frac{\gamma_0}{k_{A_i}^t} \varepsilon_{ij} P_j \cong \gamma_0 k_{A_i}^{(1-t)} P_e \text{ and } \sum_{j=1}^{S_A} \gamma_{ij}^{(P)} A_j = \sum_{j=1}^{S_A} \frac{\gamma_0}{k_{P_i}^t} \varepsilon_{ij} A_j \cong \gamma_0 k_{P_i}^{(1-t)} A_e, \quad \text{(S4.7)}$$

and calculate the average mutualistic interacting strength in the system through one of the following three averaging methods [1]: unweighted, degree weighting, and eigenvector weighting. Because of the complex topology of real-world mutualistic networks, we focus on the eigenvector weighting method. In particular, note that k_{P_i} and k_{A_i} are the numbers of the mutualistic interacting links associated with plant species P_i and pollinator species A_i, respectively. By the eigenvalue method, we calculate the averaging quantities for pollinator and plant species based on the eigenvector associated with the largest eigenvalue of the projection networks. Since abundance management is on to maintain the abundance of a single pollinator at a constant value, we exclude this species from the averaging process. Letting M_P and M_A be the projection matrices of the plants and pollinators, respectively, we have

$$M_P = M^T \times M,\ V_P = \text{eigenvector}(M_P) \text{ and } M_A = M \times M^T,\ V_A = \text{eigenvector}(M_A), \quad \text{(S4.8)}$$

where M is the $m \times n$ matrix characterizing the original bipartite network with m and n being the numbers of pollinator and plant species, V_P and V_A are the components of the eigenvector associated with the largest eigenvalue of M_P and M_A, respectively. We get

$$\langle \gamma_P \rangle = \frac{\sum_{i=1}^{S_P} \gamma_0 k_{P_i}^{1-t} \times V_P^{(i)}}{\sum_{i=1}^{S_A} V_P^{(i)}} \text{ and } \langle \gamma_A \rangle = \frac{\sum_{i=1}^{S_A} \gamma_0 k_{A_i}^{1-t} \times V_A^{(i)}}{\sum_{i=1}^{S_A} V_A^{(i)}}, \quad \text{(S4.9)}$$

where $V_P^{(i)}$ and $V_A^{(i)}$ are the i^{th} component of V_P and V_A, respectively. Let $\langle \gamma_P \rangle$ and $\langle \gamma_A \rangle$ be the effective mutualistic parameters for the plant and pollinator species in the absence of abundance management, respectively. Management will generate a change in these parameters:

$$\triangle \langle \gamma_P \rangle = \frac{\sum_{i=1}^{S_P} A_S \gamma_0 k_{P_i}^{-t} \times V_P^{(i)}}{\sum_{i=1}^{S_A} V_P^{(i)}} \quad \text{(S4.10)}$$

where A_S is the constant abundance value for the managed pollinator.

V. UNSTABLE STEADY STATE SOLUTION FOR PREDICTING THE RECOVERY POINT

The steady state solutions of the reduced model can be obtained by setting $dP_e/dt = 0$ and $dA_e/dt = 0$, which gives

$$f(P', A') = \alpha P' - \beta P'^2 + \frac{\langle \gamma_P \rangle A'}{1 + h\langle \gamma_P \rangle A'} P' + \mu = 0, \quad \text{(S5.11)}$$

$$g(P', A') = \alpha A' - \beta A'^2 + \frac{\langle \gamma_A \rangle P'}{1 + h\langle \gamma_A \rangle P'} A' + \mu = 0,$$

where A' and P' are the effective pollinator and plant abundances in the steady state, respectively. The Jacobian matrix associated with a steady-state solution is

$$J = \begin{bmatrix} \alpha - 2P'\beta + \frac{\langle\gamma_P\rangle A'}{1+h\langle\gamma_P\rangle A'} & -\frac{h\langle\gamma_P\rangle^2 A'P'}{(1+h\langle\gamma_P\rangle A')^2} + \frac{\langle\gamma_P\rangle P'}{1+h\langle\gamma_P\rangle A'} \\ -\frac{h\langle\gamma_A\rangle^2 A'P'}{(1+h\langle\gamma_A\rangle P')^2} + \frac{\langle\gamma_A\rangle A'}{1+h\langle\gamma_A\rangle P'} & \alpha - 2A'\beta - \kappa + \frac{\langle\gamma_A\rangle p'}{1+h\langle\gamma_A\rangle P'} \end{bmatrix}. \tag{S5.12}$$

The solutions of Eq. (S5.11) are

$$\begin{aligned} P' &= \frac{-(\alpha + \frac{\langle\gamma_P\rangle A'}{1+h\langle\gamma_P\rangle A'}) \pm [(\alpha + \frac{\langle\gamma_P\rangle A'}{1+h\langle\gamma_P\rangle A'})^2 + 4\beta\mu]^{1/2}}{-2\beta}, \\ A' &= \frac{-(\alpha - \kappa + \frac{\langle\gamma_A\rangle P'}{1+h\langle\gamma_A\rangle P'}) \pm [(\alpha - \kappa + \frac{\langle\gamma_A\rangle P'}{1+h\langle\gamma_A\rangle P'})^2 + 4\beta\mu]^{1/2}}{-2\beta}. \end{aligned} \tag{S5.13}$$

In general, we have $|\alpha| \gg \mu$. The physically meaningful solutions of A' and P' have positive values. We have $\beta\mu \ll |\alpha + \langle\gamma_P\rangle A'/(1+h\langle\gamma_P\rangle A')|$ or $|\alpha - \kappa + \langle\gamma_A\rangle P'/(1+h\langle\gamma_A\rangle P')|$. The approximate solutions of P' and A' are

$$\begin{aligned} P' &\approxeq \frac{-(\alpha + \frac{\langle\gamma_P\rangle A'}{1+h\langle\gamma_P\rangle A'}) \pm (|\alpha + \frac{\langle\gamma_P\rangle A'}{1+h\langle\gamma_P\rangle A'}| + 2\beta\mu)}{-2\beta}, \\ A' &\approxeq \frac{-(\alpha - \kappa + \frac{\langle\gamma_A\rangle P'}{1+h\langle\gamma_A\rangle P'}) \pm (|\alpha - \kappa + \frac{\langle\gamma_A\rangle P'}{1+h\langle\gamma_A\rangle P'}| + 2\beta\mu)}{-2\beta}. \end{aligned} \tag{S5.14}$$

For $\alpha + \langle\gamma_P\rangle A'/(1+h\langle\gamma_P\rangle A') > 0$, we have the following two approximate solutions of P':

$$\begin{aligned} P'_1 &\approxeq -\mu, \\ P'_2 &\approxeq \left[\alpha + \frac{\langle\gamma_P\rangle A'}{1+h\langle\gamma_P\rangle A'}\right]\beta^{-1}, \end{aligned} \tag{S5.15}$$

where P'_1 corresponds to the result in Eq. (S5.14) with the plus sign and P'_2 with the minus sign. Steady state solutions A'_1 and A'_2 can be obtained accordingly. For $\alpha + \langle\gamma_P\rangle A'/(1+h\langle\gamma_P\rangle A') < 0$, we have

$$\begin{aligned} P'_1 &\approxeq \left[\alpha + \frac{\langle\gamma_P\rangle A'}{1+h\langle\gamma_P\rangle A'}\right]\beta^{-1}, \\ P'_2 &\approxeq \mu. \end{aligned} \tag{S5.16}$$

For $\alpha - \kappa + \langle\gamma_A\rangle P'/(1+h\langle\gamma_A\rangle P') > 0$, we have

$$\begin{aligned} A'_1 &\approxeq -\mu, \\ A'_2 &\approxeq \left[\alpha - \kappa + \frac{\langle\gamma_A\rangle P'}{1+h\langle\gamma_A\rangle P'}\right]\beta^{-1}. \end{aligned} \tag{S5.17}$$

For $\alpha-\kappa+\langle\gamma_A\rangle P'/(1+h\langle\gamma_A\rangle P')<0$, we have

$$A_1' \approxeq \left[\alpha-\kappa+\frac{\langle\gamma_A\rangle P'}{1+h\langle\gamma_A\rangle P'}\right]\beta^{-1}, \tag{S5.18}$$
$$A_2' \approxeq \mu.$$

We consider the parameter regime in which the mutualistic system exhibits a tipping point. For initial state with high abundances, we have $\alpha-\kappa+\langle\gamma_A\rangle P'/(1+h\langle\gamma_A\rangle P')>0$ and $\alpha+\langle\gamma_P\rangle A'/(1+h\langle\gamma_P\rangle A')>0$, in the parameter region where the abundance values are relatively large, i.e., before the occurrence of a tipping point. In this case, the steady state solutions are given by Eqs. (S5.15) and (S5.17). The physically meaningful steady-state solutions are given by

$$P' = \left[\alpha+\frac{\langle\gamma_P\rangle A'}{1+h\langle\gamma_P\rangle A'}\right]\beta^{-1}, \tag{S5.19}$$
$$A' = \left[\alpha-\kappa+\frac{\langle\gamma_A\rangle P'}{1+h\langle\gamma_A\rangle P'}\right]\beta^{-1}.$$

The solution of Eq. (S5.19) can be conveniently expressed in terms of the following algebraic equation for A':

$$q_1 A'^2 + q_2 A' + q_3 = 0, \tag{S5.20}$$

where

$$\begin{aligned}
q_1 &= -(\beta^2 h\langle\gamma_P\rangle + \beta h\langle\gamma_A\rangle\langle\gamma_P\rangle + \beta h^2\alpha\langle\gamma_A\rangle\langle\gamma_P\rangle),\\
q_2 &= -\beta^2 - h\alpha\beta\langle\gamma_A\rangle + h\alpha\beta\langle\gamma_P\rangle + \langle\gamma_A\rangle\langle\gamma_P\rangle\\
&\quad +2h\alpha\langle\gamma_A\rangle\langle\gamma_P\rangle + h^2\alpha^2\langle\gamma_A\rangle\langle\gamma_p\rangle\\
&\quad -\kappa(h\beta\langle\gamma_P\rangle + h\langle\gamma_A\rangle\langle\gamma_P\rangle + h^2\alpha\langle\gamma_A\rangle\langle\gamma_P\rangle),\\
q_3 &= \alpha\beta + \alpha\langle\gamma_A\rangle + h\alpha^2\langle\gamma_A\rangle - \kappa(\beta + h\alpha\langle\gamma_A\rangle),
\end{aligned}$$

which gives a stable and an unstable solutions. Substituting the unstable solution of A' into Eq. (S5.19) yields the corresponding solution of P'.

VI. STATISTICAL ANALYSIS OF THE PREDICTIVE POWER OF THE REDUCED MODEL

To demonstrate the ability of the reduced model to predict the species recovery point in the presence of abundance management, we carry out a statistic analysis for different realizations of a random mutualistic network. The results are shown in Fig. S6. The process of generating independent statistical realizations of a mutualistic network is as follows. We first generate a random mutualistic network. We then use the nestedness algorithm [3] to increase the network's degree of nestedness. When the required nestedness is reached, we obtain the desired network. The predictive power of the reduced model can be characterized by the quantity $\delta\gamma$, the difference between the numerically calculated recovery point from the full system in the presence of abundance management and that predicted by the two-dimensional reduced model. In Fig. S6, the approximate values of the mean and standard deviation of the quantity $\delta\gamma$ for panels (a-d) are $(0.075, 0.080)$, $(0.031, 0.065)$, $(0.193, 0.090)$, and $(0.287, 0.073)$, respectively. In all cases, the statistical errors are approximately the same. The small mean values of $\delta\gamma$ in panels (a) and (b) indicate that the

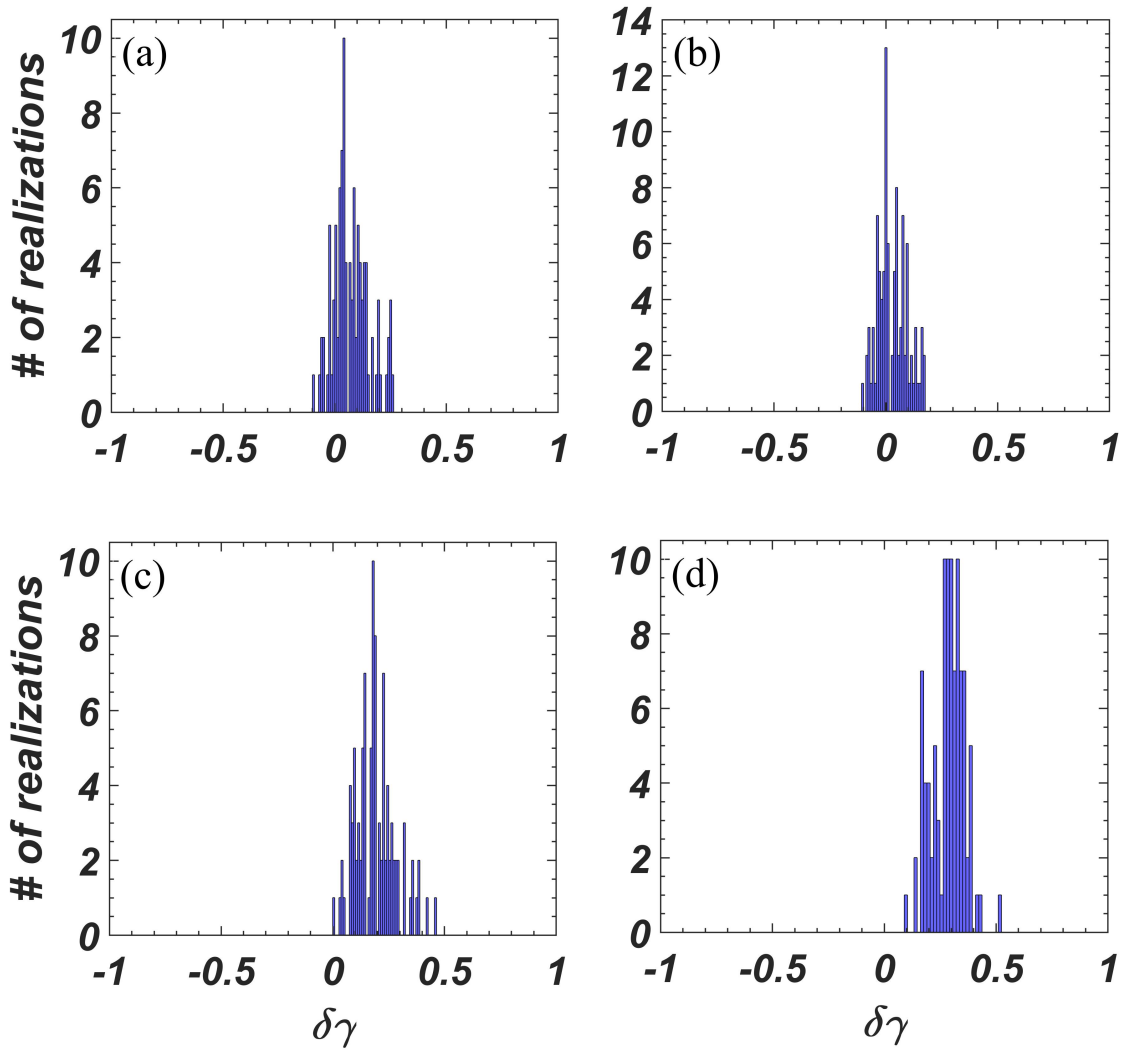

FIG. S6. *Statistical results on the ability of the reduced model to predict the species recovery point*. In all panels, the x-axis is $\delta\gamma$, the difference between the numerically calculated recovery point from the full model in the presence of abundance management and that predicted by the two-dimensional reduced model. The y-axis is the number of realizations of a random mutualistic network. Each network realization in (a) and (b) has 38 pollinators and 11 plants, and the approximate values of the connectance and nestedness are 0.25 and 0.36, respectively. Each network realization in (c) and (d) has 60 pollinators and 20 plants, and the value of the connectance is approximately 0.2. For (c) and (d), the values of nestedness are approximately 0.3 and 0.6, respectively. The control maintained abundance level is $A_S = 1.5$ for (a,c,d) and $A_S = 2$ for (b), and the managed species is the pollinator species with the largest mutualistic links to the plant species. The number of statistical realizations in all panels is 100. Other parameters have the same values as those in Fig. 1 in the main text.

reduced model is able to generate reasonably well prediction of the recovery point, but the prediction is poor for panels (c) and (d). A comparison of the results in panels (a) and (b) indicates that the value of the controlled abundance does not affect the predictive power of the reduced model.

Comparing the results in panels (a), (c), and (d), we find that the reduced model works surprisingly well for some mutualistic networks, but not so for some others. For example, the prediction is poorer for highly nested networks than for networks with a low degree of nestedness, as can be seen by comparing the results in panels (c) and (d). We can conclude that, in general, the reduced model tends to be more effective if the structure of the network is more random.

---

[1] J. Jiang, Z.-G. Huang, T. P. Seager, W. Lin, C. Grebogi, A. Hastings, and Y.-C. Lai, Proc. Natl. Acad. Sci. (USA) **115**, E639 (2018).

[2] E. H. van Nes and M. Scheffer, Amer. Nat. **164**, 255 (2004).

[3] J. J. Lever, E. H. Nes, M. Scheffer, and J. Bascompte, Ecol. Lett. **17**, 350 (2014).